

Sub-Poissonian light in fluctuating thermal-loss bosonic channels

Iliia Stepanov^{1,a}, Roman Goncharov^{1,2,3,b}, Alexei D. Kiselev^{2,4,c}

¹Quantum Information Laboratory, ITMO University, Saint Petersburg, Russia

²Laboratory for Quantum Communications, ITMO University, Saint Petersburg, Russia

³SMARTS-Quanttelecom LLC, Saint Petersburg, Russia

⁴Laboratory of Quantum Processes and Measurements, ITMO University, Saint Petersburg, Russia

^ai.stepanov@itmo.ru, ^brkgoncharov@itmo.ru, ^cadkiselev@itmo.ru

Corresponding author: I. Stepanov, i.stepanov@itmo.ru

ABSTRACT We study the photon statistics of a single-mode sub-Poissonian light propagating in the lossy thermal bosonic channel with fluctuating transmittance which can be regarded as a temperature-dependent model of the turbulent atmosphere. By assuming that the variance of the transmittance can be expressed in terms of the fluctuation strength parameter we show that the photon statistics of the light remains sub-Poissonian provided the averaged transmittance exceeds its critical value. The critical transmittance is analytically computed as a function of the input states' parameters, temperature, and the fluctuation strength. The results are applied to study special cases of the one-mode squeezed states and the odd optical Schrödinger cats.

KEYWORDS Sub-Poissonian light; fluctuations; bosonic channel

ACKNOWLEDGEMENTS This work was supported by the Russian Science Foundation (project No. 24–29–00786).

FOR CITATION Stepanov I., Goncharov R., Kiselev A.D. Sub-Poissonian light in fluctuating thermal-loss bosonic channels. *Nanosystems: Phys. Chem. Math.*, 2025, **16** (3), 333–342.

1. Introduction

The nonclassical properties of optical fields lie at the heart of quantum optics and, from its very beginning, they have been the subject of numerous intense studies. There are a number of indicators introduced to measure the quantumness (nonclassicality) of light such as negativity of the Wigner function [1], squeezing [2, 3] and sub-Poissonian statistics [4] (see also a recent review on quantumness quantifiers based on Husimi quasiprobability [5]).

Note that, for the squeezing and the sub-Poissonian statistics, the indicators are formulated in terms of second-order moments of fluctuations of the experimentally measured quantities. For nonclassical fields, these moments violate certain inequalities. For example, the sub-Poissonian light is indicated when the Fano factor, defined as the ratio of the photon number variance and the mean photon number, is less than unity.

Aside from its fundamental importance, light nonclassicality plays a vital role in quantum metrology [6]. For sub-Poissonian fields that will be our primary concern, there are various experimental techniques used to generate sub-Poissonian light [7–11] and their applications in quantum imaging are reviewed in [12] (higher-order sub-Poissonian statistics is discussed in [13, 14]). Security analysis of BB84 protocol with sub-Poissonian light sources was performed in [15]. Influence of temporal filtering of sub-Poissonian single-photon pulses on the expected secret key fraction, the quantum bit error ratio, and the tolerable channel losses is analyzed in [16].

It is well known that continuous variable quantum states of non-classical light used in quantum metrology and quantum communication protocols [17, 18] are subject to loss and added noise, leading to degradation of non-classicality and quantum correlations.

For free-space communication links [19–22], a widely used general theoretical approach to modeling environment-induced decoherence effects is based on Gaussian quantum channels with fluctuating parameters. Specifically, a pure-loss channel with fluctuating transmittance exemplifies a popular model that describes the propagation of quantum light in a turbulent atmosphere (see a review on propagation of classical electromagnetic waves through a turbulent atmosphere [23]).

This model has been extensively used to study nonclassical properties and quantum correlations of light propagating in turbulent atmospheres [24–27]. In Ref. [28], Bell inequalities in turbulent atmospheric channels are explored using the probability distribution of transmittance (PDT) in the elliptic-beam approximation with parameters suitable for the weak to moderate-turbulence channels [29]. Gaussian entanglement in turbulent atmosphere and a protocol that enables entanglement transfer over arbitrary distances [30, 31]. The evolution of higher-order non-classicality and entanglement criteria in atmospheric fluctuating-loss channels are investigated in [32]. Theory of the classical effects associated with

geometrical features of light propagation, such as beam wandering, widening, and deflection, is developed in [33, 34]. In Ref. [35], the PDT derived by numerical simulations is compared with the analytical results.

In this paper, we adapt a generalized model of the channel and use the thermal-loss channel with fluctuating transmittance to examine how the temperature effects combined with the fluctuating losses influence the sub-Poissonian light.

The paper is structured as follows. In Sec. 2 we describe a thermal-loss channel and the parameters expressed in terms of the first-order and second-order moments of the photon number used to identify sub-Poissonian light fields. In particular, we deduce the input-output relation for the q -parameter introduced as an unnormalized version of the Mandel Q -parameter. In Sec. 3 this relation is generalized to the case of the thermal-loss channel with fluctuating transmittance. After parameterization of the transmittance variance, it is shown that the output light will be sub-Poissonian only if the average transmittance exceeds its critical value. In Sec. 4 we apply the theoretical results to the special cases of squeezed states, odd optical cats and Fock states and study how the critical transmittance depends on the temperature and the strength of transmittance fluctuations. Finally, concluding remarks are given in Sec. 5.

2. Channel and moments

We consider a single-mode quantized light with the annihilation and creation operators, \hat{a} and \hat{a}^\dagger , propagating through a quantum Gaussian channel. The simplest and widely used method to describe the channel is to introduce an additional bosonic mode representing the degree of freedom of the environment and assume that the interaction between the light and noise modes is determined by the channel unitary \hat{U}_τ giving the beam splitter transformation of the form:

$$\hat{U}_\tau^\dagger \hat{a} \hat{U}_\tau \equiv \hat{a}_\tau = \sqrt{\tau} \hat{a} + \sqrt{1-\tau} \hat{b}, \quad (1)$$

where τ is the channel transmittance and \hat{b} is the annihilation operator of the noise mode.

For the temperature loss channel, the input state of the bipartite system is the product of the density matrices given by

$$\hat{\rho} = \hat{\rho}_{\text{in}} \otimes \hat{\rho}_{\text{th}}, \quad (2)$$

where $\hat{\rho}_{\text{in}}$ is the density matrix of radiation

$$\hat{\rho}_{\text{in}} = |\psi_{\text{in}}\rangle\langle\psi_{\text{in}}| \quad (3)$$

prepared in the pure state $|\psi_{\text{in}}\rangle$, whereas the environment is in the thermal state

$$\rho_{\text{th}} = \frac{1}{n_{\text{th}} + 1} \sum_{n=0}^{\infty} e^{-n\beta\hbar\omega} |n\rangle\langle n|, \quad n_{\text{th}} = \text{Tr}\{\hat{b}^\dagger \hat{b} \rho_{\text{th}}\} = \frac{1}{e^{\beta\hbar\omega} - 1}. \quad (4)$$

where $\beta = 1/(k_B T)$ is the inverse temperature parameter (k_B is the Boltzmann constant and T is the temperature), \hbar is the Planck constant, ω is the photon frequency, n_{th} is the average number of thermal photons (the mean thermal photon number).

Temporal evolution of the density matrix (2) is governed by the channel unitary (1) as follows

$$\hat{\rho}(\tau) = \hat{U}_\tau \hat{\rho} \hat{U}_\tau^\dagger. \quad (5)$$

We can now use Eqs. (1) and (5) to obtain the normally ordered characteristic function of the light as a function of the channel transmittance

$$\chi(\alpha, \tau) = \text{Tr}\{\hat{D}(\alpha) : \hat{\rho}(\tau)\} = \chi_{\text{in}}(\sqrt{\tau}\alpha) \chi_{\text{th}}(\sqrt{1-\tau}\alpha), \quad (6)$$

where $\hat{D}(\alpha) := \exp(\alpha \hat{a}^\dagger - \alpha^* \hat{a}) := \exp(\alpha \hat{a}^\dagger) \exp(-\alpha^* \hat{a})$ is the normally ordered displacement operator; χ_{in} and χ_{th} are the input and thermal characteristic functions given by

$$\chi_{\text{in}}(\alpha) = \text{Tr}\{\hat{D}(\alpha) : \hat{\rho}_{\text{in}}\}, \quad \chi_{\text{th}}(\alpha) = \text{Tr}\{\hat{D}(\alpha) : \hat{\rho}_{\text{th}}\} = \exp(-n_{\text{th}}|\alpha|^2). \quad (7)$$

Note that the form of this result reproduces the characteristic function derived by solving the thermal single-mode Lindblad equation (see, e.g., [36]) so that the beam splitter transformation representation (1) and the approach based on the Lindblad dynamics appear to be equivalent tools for modeling the temperature loss quantum channel.

Given the transmittance τ , it is not difficult to find the average photon number of the output state n_τ :

$$n_\tau = \text{Tr}\{\hat{n} \hat{\rho}(\tau)\} = \text{Tr}\{\hat{n}_\tau \hat{\rho}\} \equiv \langle \hat{n}_\tau \rangle = \tau n_{\text{in}} + (1-\tau) n_{\text{th}}, \quad (8)$$

$$n_{\text{in}} = \text{Tr}\{\hat{n} \hat{\rho}_{\text{in}}\} = \langle \psi_{\text{in}} | \hat{n} | \psi_{\text{in}} \rangle, \quad (9)$$

where $\hat{n} = \hat{a}^\dagger \hat{a}$ and $\hat{n}_\tau = \hat{a}_\tau^\dagger \hat{a}_\tau$.

Since $\hat{n}^2 - \hat{n} = \hat{a}^\dagger \hat{a}^\dagger \hat{a} \hat{a} \equiv \hat{n}^2$, the difference between the variance and the mean photon number for the quantum state $\hat{\rho}(\tau)$ can be computed as the q -parameter given by

$$q_\tau = \text{Tr}\{\hat{n}^2 : \hat{\rho}(\tau)\} - n_\tau^2. \quad (10)$$

Clearly, for $\hat{\rho}(\tau)$, the photon statistics is sub-Poissonian if and only if the parameter (10) is negative. Note that the ratio q_τ/n_τ gives the well-known Mandel Q -parameter [37], $Q_\tau^{(M)}$, introduced in Refs. [38, 39]. Note that the Q -parameter

is also related to the normalized second-order correlation function $g_\tau^{(2)}(0) = Q_\tau^{(M)}/n_\tau + 1$ and the Fano factor $F_\tau = Q_\tau^{(M)} + 1$.

We can now use the relation

$$\langle : \hat{n}_\tau^2 : \rangle = \tau^2 \langle : \hat{n}^2 : \rangle + 2(1 - \tau)^2 n_{\text{th}}^2 + 4\tau(1 - \tau)n_{\text{in}}n_{\text{th}} \quad (11)$$

derived with the help of the identity $\langle \hat{b}^\dagger \hat{b}^\dagger \hat{b} \hat{b} \rangle = 2n_{\text{th}}^2$ to deduce the explicit expression for the parameter (10)

$$q_\tau = \langle : \hat{n}_\tau^2 : \rangle - n_\tau^2 = \tau^2 q_{\text{in}} + (1 - \tau)^2 n_{\text{th}}^2 + 2\tau(1 - \tau)n_{\text{in}}n_{\text{th}}, \quad (12)$$

where

$$q_{\text{in}} = \text{Tr}\{ : \hat{n}^2 : \rho_{\text{in}} \} - n_{\text{in}}^2 = \langle : \hat{n}^2 : \rangle - n_{\text{in}}^2. \quad (13)$$

In the zero-temperature limit with $n_{\text{th}} = 0$, formula (12) shows that losses cannot destroy the sub-Poissonian statistics of input light. The latter is generally no longer the case at non-zero temperatures. In the subsequent section, we will discuss the conditions for negativity of the parameter q_τ .

3. Fluctuating losses and critical transmittance

Now we extend the results of the preceding section to the case where the transmittance fluctuates and thus should be treated as a random variable. In this case, the output density matrix takes the generalized form:

$$\hat{\rho}_{\text{out}} = \int_0^1 P(\tau) \hat{\rho}(\tau) d\tau, \quad (14)$$

where $P(\tau)$ is the probability density function (PDF) of the transmittance. We can use Eqs. (8) and (5) with $\hat{\rho}(\tau)$ replaced by $\hat{\rho}_{\text{out}}$ to introduce the output parameter q_{out} as follows

$$q_{\text{out}} = \text{Tr}\{ : \hat{n}^2 : \hat{\rho}_{\text{out}} \} - \text{Tr}\{ \hat{n} \hat{\rho}_{\text{out}} \}^2 = \langle \langle : \hat{n}_\tau^2 : \rangle \rangle_\tau - \langle n_\tau \rangle_\tau^2 = \langle q_\tau \rangle_\tau + [\langle n_\tau^2 \rangle_\tau - \langle n_\tau \rangle_\tau^2], \quad (15)$$

where $\langle \dots \rangle_\tau = \int_0^1 \dots P(\tau) d\tau$. After substituting formulas (8) and (10) into Eq. (15), we obtain the parameter q_{out} in the following explicit form:

$$q_{\text{out}} = \bar{\tau}^2 (q_{\text{in}} - n_{\text{in}}^2) + (\bar{\tau}n_{\text{in}} + (1 - \bar{\tau})n_{\text{th}})^2 + \text{Var}(\tau) \{ q_{\text{in}} - n_{\text{in}}^2 + 2(n_{\text{in}} - n_{\text{th}})^2 \}, \quad (16)$$

where $\bar{\tau} = \langle \tau \rangle_\tau$ is the averaged transmittance and $\text{Var}(\tau) = \langle \tau^2 \rangle_\tau - \bar{\tau}^2$ is the variance of the transmittance.

Since the transmittance varies from zero to unity, $0 \leq \tau \leq 1$, and the variance $\text{Var}(\tau)$ cannot be negative, $\text{Var}(\tau) \geq 0$, the mean of the squared transmittance cannot exceed the average transmittance and must satisfy the condition: $\bar{\tau}^2 \leq \langle \tau^2 \rangle_\tau \leq \bar{\tau}$. As a result, the variance is bounded from above by the product $(1 - \bar{\tau})\bar{\tau}$: $0 \leq \text{Var}(\tau) \leq (1 - \bar{\tau})\bar{\tau}$. In our model, we assume that $\langle \tau^2 \rangle_\tau = F\bar{\tau} + (1 - F)\bar{\tau}^2$, so that the variance takes the following form

$$\text{Var}(\tau) = \langle \tau^2 \rangle_\tau - \bar{\tau}^2 = F(1 - \bar{\tau})\bar{\tau} \quad (17)$$

where $0 \leq F \leq 1$ is the parameter characterizing the strength of fluctuations.

In what follows, we shall treat the fluctuation strength F as a phenomenological parameter which is independent of $\bar{\tau}$. The variance representation (17) can now be used to express the q -parameter (16) in terms of $\bar{\tau}$ as follows

$$q_{\text{out}}(\bar{\tau}) = \bar{\tau}^2 (q_{\text{in}} - a) + \bar{\tau}(a - n_{\text{th}}^2) + n_{\text{th}}^2, \quad (18)$$

where

$$a = 2n_{\text{in}}n_{\text{th}} - n_{\text{th}}^2 + gF, \quad g = q_{\text{in}} - n_{\text{in}}^2 + 2(n_{\text{in}} - n_{\text{th}})^2. \quad (19)$$

In the limiting case of transparent medium described by the identity channel with $\bar{\tau} = 1$, the q -parameter is equal to its initial value q_{in} given by Eq. (13). For sub-Poissonian light, the parameter q_{in} is negative, so that $q_{\text{out}}(1) = q_{\text{in}} < 0$. In the opposite case with vanishing transmittance, $\bar{\tau} = 0$, from Eq. (18), the q -parameter is positive, $q_{\text{out}}(0) = n_{\text{th}}^2 > 0$. Clearly, this implies that the transmitted light will remain sub-Poissonian provided the average transmittance exceeds its critical value: $\bar{\tau} > \tau_c$.

From Eq. (18), it is not difficult to find the analytical expression for the critical transmittance (the transmittance threshold). So, we deduce the inequality

$$\bar{\tau} > \tau_c = - \frac{(a - n_{\text{th}}^2) + \sqrt{(a + n_{\text{th}}^2)^2 - 4n_{\text{th}}^2 q_{\text{in}}}}{2(q_{\text{in}} - a)} \quad (20)$$

giving the condition that effects of transmittance fluctuations and temperature fail to destroy the sub-Poissonian statistics of light and the q -parameter of the transmitted (output) light is negative, $q_{\text{out}} < 0$.

We conclude this section with the remark on two important special cases with $T = 0$ and $F = 0$, respectively. In the zero-temperature limit, the expression of the transmittance threshold is simplified as follows

$$\tau_c|_{T=0} = \frac{F(q_{in} + n_{in}^2)}{F(q_{in} + n_{in}^2) - q_{in}}, \tag{21}$$

whereas the critical transmittance for the case, where fluctuations of the transmittance are negligible, is given by

$$\tau_c|_{F=0} = \frac{n_{th}}{n_{th} + \sqrt{n_{in}^2 - q_{in} - n_{in}}}. \tag{22}$$

Clearly, when F and T are both vanishing, the critical transmittance is zero. This is the well-known case of non-fluctuating pure-loss bosonic channel where $q_{out} = \tau^2 q_{in}$ (see Eq. (12) with $n_{th} = 0$).

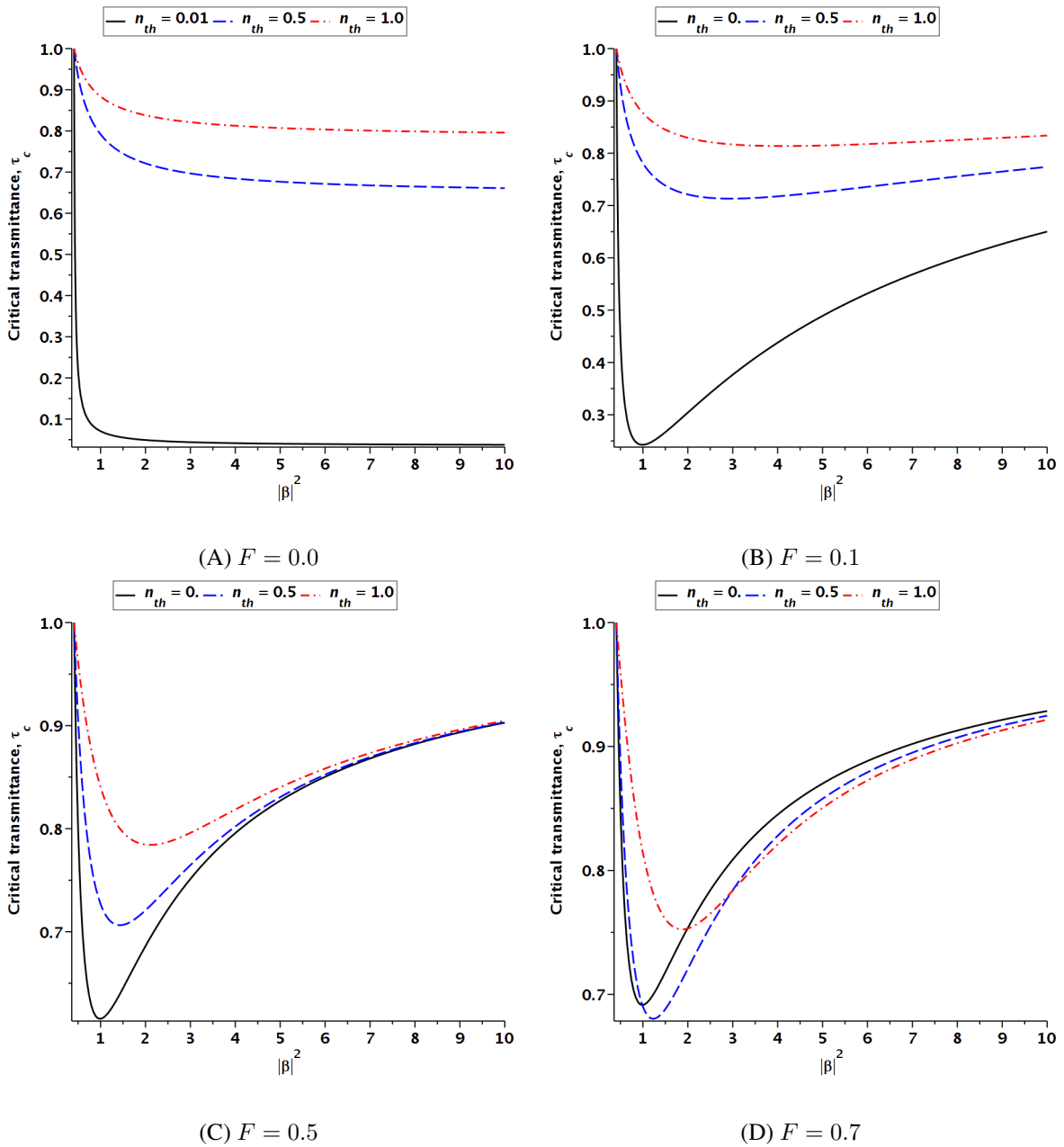


FIG. 1. Dependence of the critical transmittance τ_c on the square of the displacement amplitude, $|\beta|^2$, for the squeezed state (23) computed at different values of the fluctuation strength parameter F for $r = 0.4$ and $\phi = \pi/2$

4. Effects of fluctuations and temperature

In this section, we apply our analytical results to the two special cases of input states: the displaced squeezed states and the odd Schrödinger cat states. More specifically, we shall study how the temperature and transmittance fluctuations influence the transmittance threshold for these states.

4.1. Squeezed light

The density matrix

$$\hat{\rho}_{\text{in}} = |\psi_{\text{sq}}\rangle\langle\psi_{\text{sq}}|, \quad |\psi_{\text{sq}}\rangle = \hat{D}(\beta)\hat{S}(\xi)|0\rangle \quad (23)$$

describes the case of displaced squeezed vacuum states expressed using the squeezing operator, $\hat{S}(\xi)$, and the displacement operator, $\hat{D}(\beta)$, given by

$$\hat{S}(\xi) = e^{(\xi(\hat{a}^\dagger)^2 - \xi^* \hat{a}^2)/2}, \quad \hat{D}(\beta) = e^{\beta \hat{a}^\dagger - \beta^* \hat{a}}, \quad (24)$$

$\xi = r e^{i\psi}$ is the squeezing parameter and $\beta = |\beta| e^{i\theta}$ is the displacement. For the squeezed state (23), it is rather straightforward to derive the expressions for the parameters $n_{\text{in}} = n_{\text{sq}}$ and $q_{\text{in}} = q_{\text{sq}}$ that enter the expression for the critical transmittance (20):

$$n_{\text{sq}} = |\beta|^2 + \sinh^2 r, \quad q_{\text{sq}} = q_2 |\beta|^2 + \sinh^2 r \cosh 2r, \quad (25)$$

where $q_2 = 2 \sinh^2 r + \sinh 2r \cos(2\phi)$ and $\phi = \theta - \psi/2$.

From formula (25), the case where the photon statistics of the squeezed light is sub-Poissonian with negative parameter q_{sq} may occur only when the coefficient q_2 is negative. The latter requires the angle ϕ and the squeezing parameter r to meet the inequality

$$|\tan \phi| > e^r, \quad (26)$$

so that the squeezed light will be sub-Poissonian only when the squared displacement amplitude is above its critical value:

$$|\beta|^2 > \frac{e^r \sinh r \cosh 2r}{2(\sin^2 \phi - e^{2r} \cos^2 \phi)} \equiv \beta_c^2. \quad (27)$$

Clearly, when $\cos \phi = 0$, the condition (26) is always fulfilled and β_c takes the minimal value that grows with r .

In Figs. 1 and 2, the threshold transmittance is plotted against the squared displacement amplitude, $|\beta|^2$, at $\phi = \pi/2$. The numerical results for τ_c are evaluated using Eq. (20) with formula (25) giving the mean photon number n_{in} and the q -parameter q_{in} .

At $|\beta| = \beta_c$, the q -parameter vanishes, and thus the threshold transmittance equals unity. So, in the close vicinity of β_c , the transmittance τ_c drops as $|\beta|^2$ increases.

From Eq. (22), it is not difficult to show that, when fluctuations are negligible, τ_c monotonically decreases with $|\beta|^2$ approaching the value $n_{\text{th}}/(n_{\text{th}} - q_2/2)$ (see Fig. 1a). By contrast, from the relation (21) describing the zero-temperature case, in the large displacement limit, the critical transmittance approaches unity. As a result, the $|\beta|^2$ -dependence of τ_c reveals nonmonotonic behaviour illustrated in Fig. 2a. It can also be seen that such behaviour where the critical transmittance exhibits a local minimum occurs at non-vanishing temperatures provided $F \neq 0$.

Normally, it is expected that the threshold will get higher at elevated temperatures. This is the case for the curves shown in Figs. 1a–1c.

Interestingly, in the case of intense fluctuations with sufficiently high values of fluctuation strength, the latter is no longer the case. From Figure 1 which shows the τ_c -vs- $|\beta|^2$ curves computed at $F = 0.7$, it is seen that the long displacement part of the zero-temperature curve appears to be above the curves with non-zero n_{th} .

Similarly, the threshold is expected to increase with the fluctuation strength F . It is not difficult to show that the threshold τ_c grows with F only if the coefficient g given by Eq. (19) is positive. According to formula (19), this coefficient quadratically depends on n_{th} and it takes negative values within the interval:

$$n_- < n_{\text{th}} < n_+, \quad n_{\pm} = n_{\text{in}} \pm \sqrt{\frac{n_{\text{in}}^2 - q_{\text{in}}}{2}}. \quad (28)$$

So, in the low temperature region where $n_{\text{th}} < n_-$ the critical transmittance is an increasing function of the fluctuation strength. The curves presented in Figs. 2a–2b provide support to this conclusion.

For the cases of elevated temperatures illustrated in Figs. 2c–2d, the short displacement part of the curves where n_{th} meets the condition (28) is arranged differently. In this part, the curve with negligibly small fluctuations determines the largest value of τ_c . Note that all the curves shown in Figs. 2c–2d intersect at the point where the coefficient g vanishes with $n_{\text{th}} = n_-$.

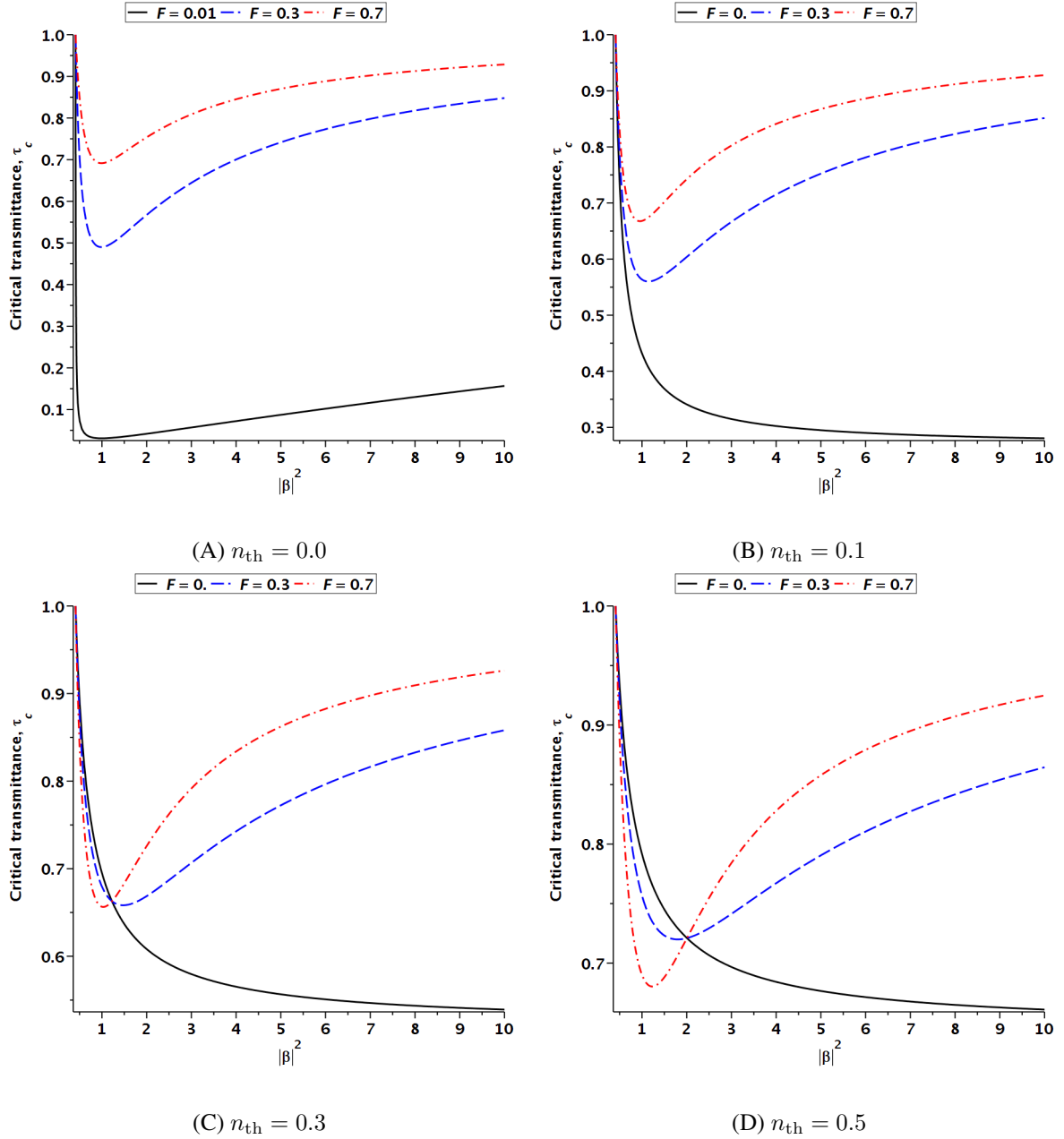


FIG. 2. Dependence of the critical transmittance τ_c on the square of the displacement amplitude, $|\beta|^2$, for the squeezed state (23) with $r = 0.4$ and $\phi = \pi/2$ computed at different values of the mean thermal photon number n_{th}

4.2. Odd optical cats

Similar to the case of squeezed states, formulas

$$\hat{\rho}_{in} = |\psi_{cat}\rangle\langle\psi_{cat}|, \quad |\psi_{cat}\rangle = \frac{1}{\sqrt{2(1 - e^{-2|\beta|^2})}}(|\beta\rangle - |-\beta\rangle), \quad (29)$$

$$n_{cat} = |\tilde{\beta}|^2 \cosh |\beta|^2, \quad q_{cat} = -|\tilde{\beta}|^4, \quad (30)$$

where $|\tilde{\beta}|^2 = \frac{|\beta|^2}{\sinh |\beta|^2}$, present the analytical results needed to evaluate the critical transmittance for the odd (antisymmetric) cat states, $|\psi_{cat}\rangle$.

In Fig. 3 we show how the fluctuation strength affects the $|\beta|^2$ -dependencies of the critical transmittance at different temperatures. From Eq. (22), in the weak fluctuation limit with $F = 0$ (see Fig. 3a), the starting value of τ_c is $n_{th}/(n_{th} + \sqrt{2} - 1)$ and it monotonically increases approaching unity. By contrast to the case of the squeezed states, for the odd optical cats, all the curves shown in Figs. 3 and 4 reveal similar behaviour. Similar to the squeezed states, it turned out that, at

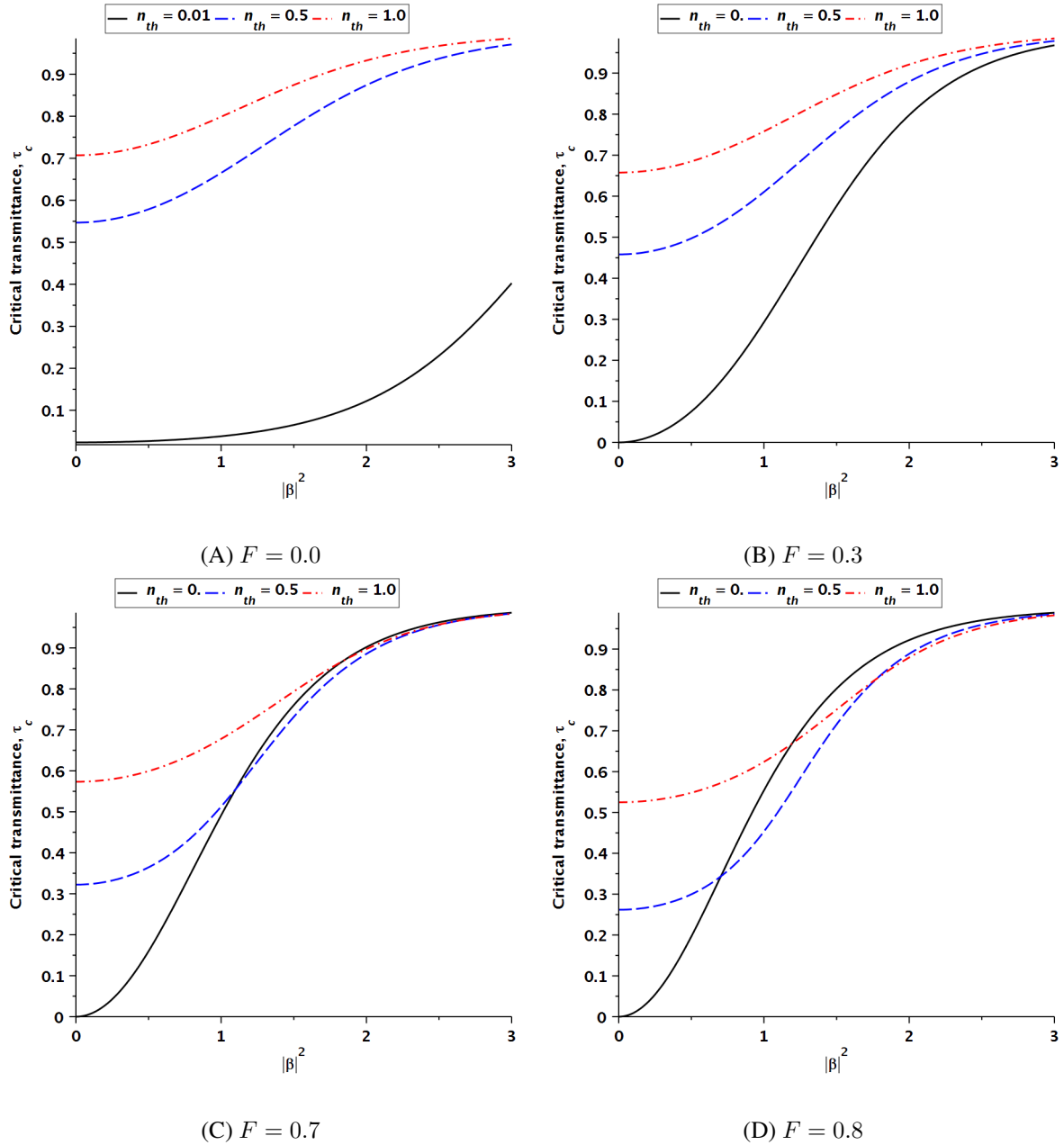


FIG. 3. Dependence of the critical transmittance τ_c on the square of the displacement amplitude, $|\beta|^2$, for the odd cat state (29) computed at different values of the fluctuation strength parameter F

sufficiently strong fluctuations (sufficiently large fluctuation strength F) and sufficiently large $|\beta|^2$, the zero-temperature curve gives the largest value of τ_c .

Figure 4 presents the graphs illustrating the temperature induced effects. Since, in the limiting case of a single photon state with $\beta = 0$, the mean photon number n_{cat} is unity and $q_{\text{cat}} = -1$, all the zero-temperature curves described by Eq. (21) start from zero (see Fig. 4a). As is depicted in Figs. 4b and 4c, at non-vanishing temperatures and sufficiently small $|\beta|$, the values of τ_c are dominated by the zero-fluctuation curve with $F = 0$ (for the single photon state, the zero-fluctuation value of τ_c is $n_{\text{th}}/(n_{\text{th}} + \sqrt{2} - 1)$). Referring to Fig. 4d, in the high temperature region with $n_{\text{th}} \geq 0.9$, the latter holds for all values of $|\beta|$.

Since in the zero amplitude limit with $\beta = 0$, the odd state (29) becomes the single-photon state $|1\rangle$, it is instructive to briefly discuss the case of the Fock states $|n\rangle$. For such states, we have $m_{\text{in}} = -n$ and $n_{\text{in}} = n$. So, at low temperatures with $n_{\text{th}} < n_- = n - \sqrt{n(n+1)}/2$, an increase in F will enhance the threshold. Interestingly, in the special case with $n = 1$, we have $n_- = 0$. As a result, all the curves in Fig. 4a start from the zero and, in Figs. 4b–4d, the thresholds at $\beta = 0$ are below the zero-fluctuation value of τ_c : $n_{\text{th}}/(n_{\text{th}} + \sqrt{2} - 1)$.

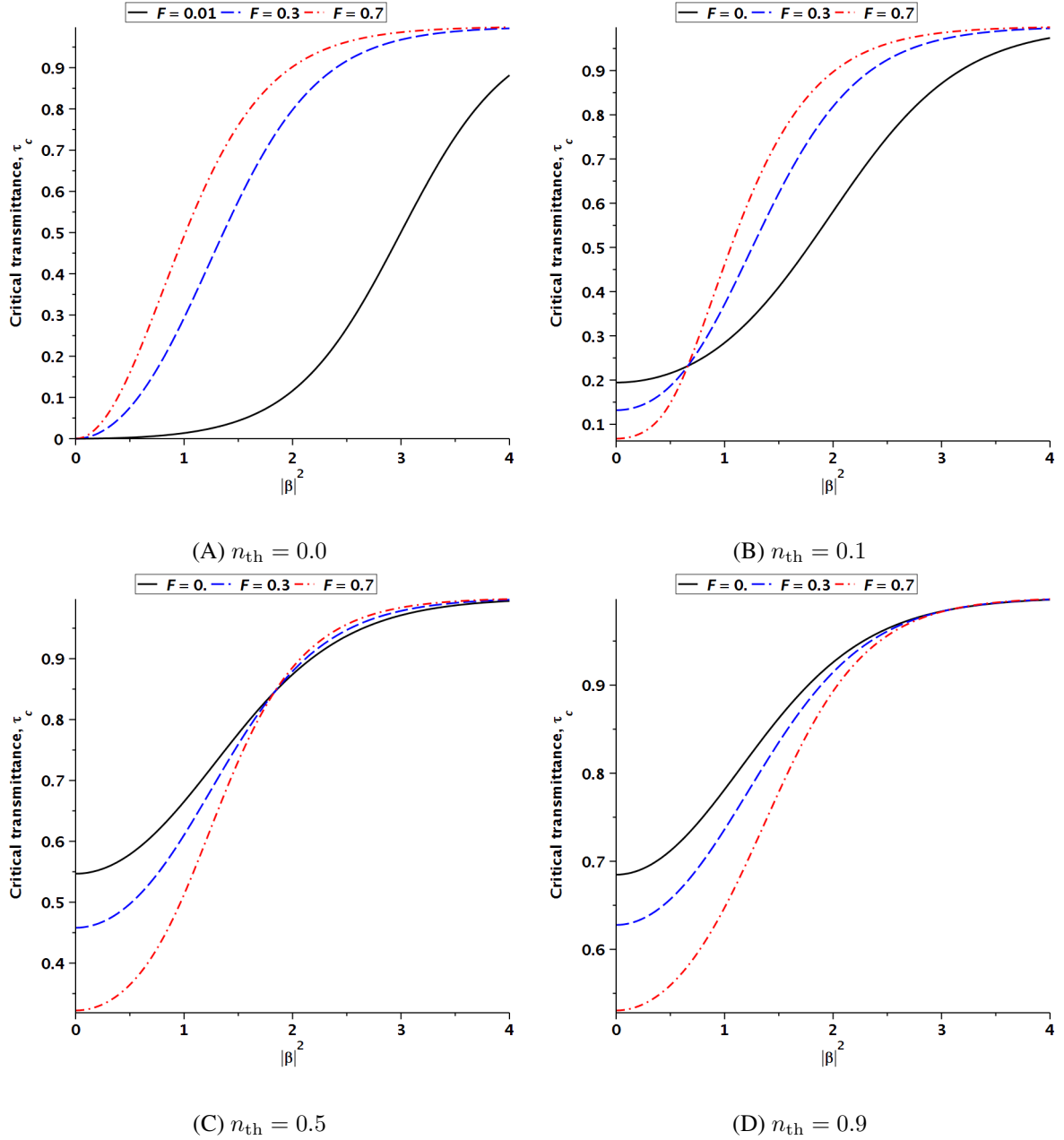


FIG. 4. Dependence of the critical transmittance τ_c on the square of the displacement amplitude, $|\beta|^2$, for the odd cat state (see Eq. (29)) computed at different values of the mean thermal photon number n_{th}

5. Conclusions

In this paper, we have studied effects of the thermal-loss channel with fluctuating transmittance on the sub-Poissonian light whose non-classicality is characterized by the q -parameter (see Eq. (10)). We have combined the input-output relation for the q -parameter (16) with the variance of the transmittance parameterized using the fluctuation strength parameter (17) to show that the condition for sub-Poissonian statistics of photon at the channel output is determined by the critical transmittance (20). For the cases of the displaced squeezed state (see Eq. (23)) and the odd optical cat state (see Eq. (29)), the critical transmittance is computed as a function of the squared displacement amplitude, $|\beta|^2$, at different values of temperature and the fluctuation parameter. In contrast to what is expected, under certain conditions, an increase in either the fluctuation strength or the temperature may result in a decrease in the critical transmittance.

Note that the key point greatly simplifying our analysis is the parameterization of the transmittance variance (17), where the fluctuation strength F is introduced as a phenomenological parameter which is independent of the mean transmittance $\bar{\tau}$. A more sophisticated treatment of the atmospheric channels [29, 33, 35] requires computing the first-order and second-order moments of the transmittance, $\langle \tau \rangle = \bar{\tau}$ and $\langle \tau^2 \rangle = \bar{\tau}^2$, from the correlation functions derived using the phase approximation of the Huygens-Kirchhoff method [40, 41].

References

- [1] Kenfack A. and Zyczkowski K. Negativity of the Wigner function as an indicator of non-classicality. *Journal of Optics B: Quantum and Semiclassical Optics*, 2004, **6**(10), P. 396.
- [2] Teich M.C. and Saleh B.E.A. Squeezed state of light. *Quantum Optics: Journal of the European Optical Society Part B*, 1989, **1**(2), P. 153–191.
- [3] Lvovsky A.I. *Squeezed Light*, ch. 5, P. 121–163. John Wiley & Sons, Ltd, 2015.
- [4] Davidovich L. Sub-Poissonian processes in quantum optics. *Rev. Mod. Phys.*, 1996, **68**, P. 127–173.
- [5] Goldberg A.Z., Klimov A.B., Grassl M., Leuchs G., and Sánchez-Soto L.L. Extremal quantum states. *AVS Quantum Science*, 2020, **2**(4), P. 044701.
- [6] Tan K.C. and Jeong H. Nonclassical light and metrological power: An introductory review. *AVS Quantum Science*, 2019, **1**(1) P. 014701.
- [7] Li R.-D., Choi S.-K., Kim C., and Kumar P. Generation of sub-Poissonian pulses of light. *Phys. Rev. A*, 1995, **51**, P. R3429–R3432.
- [8] Peřina J., Michálek V., Machulka R., and Haderka O. Two-beam light with simultaneous anticorrelations in photon-number fluctuations and sub-Poissonian statistics. *Phys. Rev. A*, 2021, **104**, P. 013712.
- [9] Iskhakov T.S., Usenko V.C., Andersen U.L., Filip R., Chekhova M.V., and Leuchs G. Heralded source of bright multi-mode mesoscopic sub-Poissonian light. *Opt. Lett.*, 2016, **41**, P. 2149–2152.
- [10] Lal N., Shajilal B., Anwar A., Perumangatt C., and Singh R.P., Observing sub-Poissonian statistics of twisted single photons using oscilloscope. *Review of Scientific Instruments*, 2019, **90**(11), P. 113104.
- [11] Samedov V.V. Discovery of sub-Poissonian statistics of light photons in scintillators that did not take place. *Physics of Atomic Nuclei*, 2019, **84**(11), P. 2048–2054.
- [12] Berchera I.R. and Degiovanni I.P. Quantum imaging with sub-Poissonian light: challenges and perspectives in optical metrology. *Metrologia*, 2019, **56**, P. 024001.
- [13] Erenso D., Vyas R., and Singh S. Higher-order sub-Poissonian photon statistics in terms of factorial moments. *J. Opt. Soc. Am. B*, 2002, **19**, P. 1471–1475.
- [14] Peřina J., Michálek V., and Haderka O. Higher-order sub-Poissonian-like nonclassical fields: Theoretical and experimental comparison. *Phys. Rev. A*, 2017, **96**, P. 033852.
- [15] Waks E., Santori C., and Yamamoto Y. Security aspects of quantum key distribution with sub-Poisson light. *Phys. Rev. A*, 2002, **66**, P. 042315.
- [16] Kupko T., M. von Helversen, Rickert L., Schulze J.-H., Strittmatter A., Gschrey M., Rodt S., Reitzenstein S., and Heindel T. Tools for the performance optimization of single-photon quantum key distribution. *npj Quantum Information*, 2020, **6**(1), P. 29.
- [17] Pirandola S., Andersen U.L., Banchi L., Berta M., Bunandar D., Colbeck R., Englund D., Gehring T., Lupo C., Ottaviani C., Pereira J.L., Razavi M., Shaari J.S., Tomamichel M., Usenko V.C., Vallone G., Villoresi P., and Wallden P., Advances in quantum cryptography. *Adv. Opt. Photon.*, 2020, **12**, P. 1012–1236.
- [18] Goncharov R.K., Kiselev A.D., Samsonov E.O., and Egorov V.I. Continuous-variable quantum key distribution: security analysis with trusted hard-ware noise against general attacks. *Nanosystems: Physics, Chemistry, Mathematics*, 2022, **13**, P. 372–391.
- [19] Peuntinger C., Heim B., Müller C.R., Gabriel C., Marquardt C., and Leuchs G. Distribution of squeezed states through an atmospheric channel. *Phys. Rev. Lett.*, 2014, **113**, P. 060502.
- [20] Heim B., Peuntinger C., Killoran N., Khan I., Wittmann C., Marquardt C., and Leuchs G. Atmospheric continuous-variable quantum communication. *New Journal of Physics*, 2014, **16**, P. 113018.
- [21] Derkach I., Usenko V.C., and Filip R. Squeezing-enhanced quantum key distribution over atmospheric channels. *New Journal of Physics*, 2020, **22**, P. 053006.
- [22] Pirandola S. Limits and security of free-space quantum communications. *Phys. Rev. Res.*, 2021, **3**, P. 013279.
- [23] Kravtsov Y.A. Propagation of electromagnetic waves through a turbulent atmosphere. *Reports on Progress in Physics*, 1992, **55**, P. 39–112.
- [24] Milonni P.W., Carter J.H., Peterson C.G., and Hughes R.J. Effects of propagation through atmospheric turbulence on photon statistics. *Journal of Optics B: Quantum and Semiclassical Optics*, 2004, **6**, P. S742.
- [25] Kiesel T., Vogel W., Parigi V., Zavatta A., and Bellini M. Experimental determination of a nonclassical Glauber-Sudarshan P function. *Phys. Rev. A*, 2008, **78**, P. 021804.
- [26] Semenov A.A. and Vogel W. Quantum light in the turbulent atmosphere. *Phys. Rev. A*, 2009, **80**, P. 021802.
- [27] Vasylyev D.Y., Semenov A.A., and Vogel W. Toward global quantum communication: Beam wandering preserves nonclassicality. *Phys. Rev. Lett.*, 2012, **108**, P. 220501.
- [28] Gumberidge M.O., Semenov A.A., Vasylyev D., and Vogel W., Bell nonlocality in the turbulent atmosphere. *Phys. Rev. A*, 2016, **94**, P. 053801.
- [29] Vasylyev D., Semenov A.A., and Vogel W. Atmospheric quantum channels with weak and strong turbulence. *Phys. Rev. Lett.*, 2016, **117**, P. 090501.
- [30] Bohmann M., Semenov A.A., Sperling J., and Vogel W. Gaussian entanglement in the turbulent atmosphere. *Phys. Rev. A*, 2016, **94**, P. 010302.
- [31] Avetisyan H. and Monken C.H. Higher order correlation beams in atmosphere under strong turbulence conditions. *Opt. Express*, 2016, **24**, P. 2318–2335.
- [32] Bohmann M., Sperling J., Semenov A.A., and Vogel W. Higher-order nonclassical effects in fluctuating-loss channels. *Phys. Rev. A*, 2017, **95**, P. 012324.
- [33] Vasylyev D., Vogel W., and Semenov A.A. Theory of atmospheric quantum channels based on the law of total probability. *Phys. Rev. A*, 2018, **97**, P. 063852.
- [34] Vasylyev D., Vogel W., and Moll F. Satellite-mediated quantum atmospheric links. *Phys. Rev. A*, 2019, **99**, P. 053830.
- [35] Klen M. and Semenov A.A. Numerical simulations of atmospheric quantum channels. *Phys. Rev. A*, 2023, **108**, P. 033718.
- [36] Kiselev A.D., Ali R., and Rybin A.V. Lindblad dynamics and disentanglement in multi-mode bosonic systems. *Entropy*, 2021, **23**(11), P. 1409.
- [37] Mandel L. and Wolf E. *Optical Coherence and Quantum Optics*. Cambridge, Cambridge University Press, 1995.
- [38] Mandel L. Sub-Poissonian photon statistics in resonance fluorescence. *Opt. Lett.*, 1979, **4**, P. 205–207.
- [39] Short R. and Mandel L. Observation of sub-Poissonian photon statistics. *Phys. Rev. Lett.*, 1983, **51**, P. 384–387.
- [40] Banakh V.A. and Mironov V.L. Phase approximation of the Huygens–Kirchhoff method in problems of laser-beam propagation in the turbulent atmosphere. *Opt. Lett.*, 1977, **1**(5), P. 172–174.
- [41] Banakh V.A. and Mironov V.L. Phase approximation of the Huygens–Kirchhoff method in problems of space-limited optical-beam propagation in turbulent atmosphere. *Opt. Lett.*, 1979, **4**(8), P. 259–261.

Information about the authors:

Ilya Stepanov – Quantum Information Laboratory, ITMO University, Kadetskaya Line, 3, St. Petersburg, 199034, Russia; i.stepanov@itmo.ru

Roman Goncharov – Quantum Information Laboratory, ITMO University, Kadetskaya Line, 3, St. Petersburg, 199034, Russia; Laboratory for Quantum Communications, ITMO University, Birzhevaya Line, 16, Saint Petersburg, 199034, Russia; SMARTS-Quanttelecom LLC, 6th Vasilyevskogo Ostrova Line, 59, Saint Petersburg, 199178, Russia; ORCID 0000-0002-9081-8900; rkgoncharov@itmo.ru

Alexei D. Kiselev – Laboratory for Quantum Communications, ITMO University, Birzhevaya Line, 16, Saint Petersburg, 199034, Russia; Laboratory of Quantum Processes and Measurements, ITMO University, Kadetskaya Line 3b, Saint Petersburg 199034, Russia; ORCID 0000-0002-1023-3284; adkiselev@itmo.ru

Conflict of interest: the authors declare no conflict of interest.